Pergamon

0956-7151(94)00435-8

Acta metall. mater. Vol. 43, No. 6, pp. 2157–2162, 1995

0956-7151/95 $9.50 + 0.00

EMBRYO-DAMAGE INDUCED NUCLEATION OF MICROCRACKS IN AN ALUMINIUM ALLOY UNDER IMPACT LOADING

WENSHENG HAN and YILONG BAI

LNM, Institute of Mechanics, Chinese Academy of Sciences, Beijing 100080, P.R. China

(Received 6 May 1994; in revised form 16 October 1994)

Abstract—The nucleation of microdamage under dynamic loading was investigated through planar impact experiments accomplished with a light gas gun. The microscopic observation of recovered and sectioned specimens showed that microcracks were nucleated only by cracking of brittle particles inside material. However, for comparison the *in situ* static tensile tests on the same material conducted with a scanning electron microscope showed that the microcracks were nucleated by many forms those were fracture of ductile matrix, debonding particles from matrix and cracking of brittle particles. The quantitative metallographic observations of the specimens subjected to impact loading showed that most of the cracked particles were situated on grain boundaries of the aluminium matrix. These facts suggested the concept of critical size and incubation time of submicroscopic cavities in the dynamic case and the mechanism of embryo-damage induced nucleation by fracture of brittle particles in the aluminium alloy under impact loading was proposed.

1. INTRODUCTION

One kind of failure of materials is initiated by means of nucleation of microcracks or microvoids. Some papers have studied the mechanism of nucleation of microcracks or microvoids, and treated the formation of cavities as that vacancies cluster together and nucleate a cavity under tensile stress [1]. The incubation time and critical size of the vacancies cluster are two dominant parameters in nucleation process. These concepts have been confirmed by quasi-static tests [2]. A typical dynamic failure of materials, such as spallation, usually results from accumulation of microdamage created by tensile stress waves, which form when compressive waves reflect at free surface, corners or interfaces adjacent to media with low wave impedance. Curran *et al.* [3] have revealed that spallation is produced by means of nucleation, growth and coalescence of microdamage under impact loading. According to the concentration of stress or strain induced by microscopic heterogeneities of materials under external loading, Curran *et al.* classified the nucleation of microdamage into two types. One is stress driven nucleation and the other is deformation driven nucleation. The typical feature of the stress driven mode is breaking of bonds of atoms, whereas for the deformation driven mode, the nucleation is triggered by local plastic slip under shear stress, including grain boundary slip, local plastic flow and dislocations piling up.

The basic difference between the stress driven and the deformation driven modes, we believe, is whether the motion of dislocations inside materials is resisted or not. Under planar impact loading, triaxial stress and strain rate are usually quite higher than shear stress and strain. Therefore, the main nucleation mechanism of microdamage under planar impact should be breaking of bonds, i.e. the stress driven mode.

In order to perform a direct experimental study of the nucleation of microdamage under dynamic loading, we selected an aluminium alloy as testing material, which consists of brittle particles and aluminium–copper solid–solution. The experimental observations demonstrated that most probably nucleation of microdamage was fracture of particles on grain boundaries. For comparison, the *in situ* static tensile tests on the same material conducted with a scanning electron microscope showed that the microcracks were nucleated by many forms those were fracture of ductile matrix, debonding particles from matrix and cracking of brittle particles. The acquired data and relevant calculation of timing and consumed energy of nucleation led to a probable nucleation mechanism—embryo-damage induced nucleation of microdamage.

2. THE EXPERIMENTAL RESULTS

Table 1 shows the constituents and basic property of the alloy. The samples were first heated and rolled. Then they were quenched and aged manually. The microscopic structures on a sectional surface of a virgin specimen are shown in Fig. 1. The whites are θ phase particles and the grey portions are the aluminium–copper solid–solution matrix. The

Table 1. The constituents and basic properties of test material

Constituents (wt%)	6.3% Cu, 0.3% Mo, 0.2% V, 0.18% Zr, 0.06% Ti, 92.96% Al			
Basic property	Density (g/cm^3)	Yield strength (MPa)	Ultimate strength (MPa)	Modulus of elasticity (GPa)
	2.83	333	449	81

Table 2. The micro-hardness of test material

	Average (HV)	No. 1	No. 2	No. 3	No. 4	No. 5	No. 6	No. 7
Matrix	154 ± 0	154.0	154.0	154.0	154.0			
Particles	326 ± 83	555	394	255	267	301	244	267

Vickers micro-hardness results under a 50 g load listed in Table 2 indicate that the average hardness of the particles is about 2.11 times higher than that of matrix.

We performed dynamic tests with a light gas gun. Figure 2 shows the schematic of the gun. The plate on the left is generally called as flyer, which is accelerated by high pressure gas inside the bore. During the test the flyer strikes a flat plate specimen, i.e. the target, suspended on the right. The stress and speed transducers fixed in the specimen can record actual tensile stress and impact speed. The impacted target was then recovered by a soft catcher in the tail of bore. Figure 3 shows the arrangement for the measurement of the stress profile in impact tests. The carbon gauge was embedded between the back of target and PMMA plate which was adhered to the target. The thickness of the gauge is about 50 μm. Compared with dimensions of the specimen, the thickness of the gauge is so small that the effect of the physical presence of the gauge on the stress field can be ignored. The impedance matching method of stress wave theory presents that the tensile stress and its duration can be controlled properly by the impact speed and the relative thickness of the flyer and the target respectively.

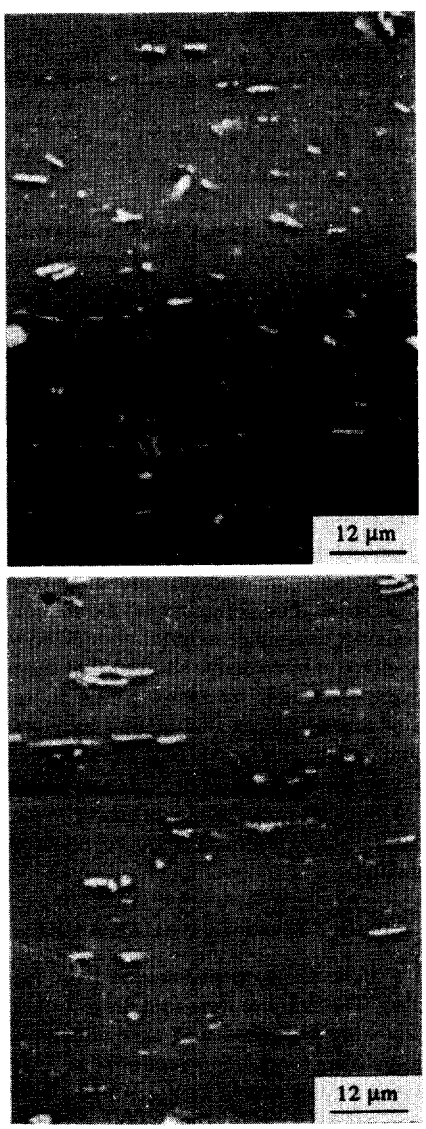

Fig. 1. The microscopic structures of test material.

Eight fields of observation, each of 0.04224 mm^2, were selected arbitrarily on a sectional surface of the specimen. Measurements obtained with a Cambridge Q-520 image analyzer show that the number density of particles on grain boundaries and inside grains are 1.0×10^3 and 2.5×10^3 per mm^2 respectively, the average equivalent diameter of particles is 3.4 μm, the nearest neighbour distance which was defined by Gurland [4] is 12.8 μm, and the average longest and shortest axes of grains are 26.1 and 6.0 μm respectively.

Three groups of experiments have been completed with the light gas gun. The speeds of nickel flyers in these tests recorded by speed transducers are 600, 420 and 400 m/s respectively. The thicknesses of the flyer and target are about 0.1 and 5 mm respectively. The corresponding tensile stresses shown by the stress transducers are 7470, 5112 and 4870 MPa and load durations were 112, 115 and 142 ns respectively. The loading durations should be the same because of the same flyer and target for each test. The difference of load duration is only due to scatters of experiments. The recovered targets were cut sectionally and polished by an automatic polishing machine. The specimens were observed with a Hitachi S-570 scanning electron microscope. Figure 4, a SEM photograph, shows that the nucleation of microcracks is only due

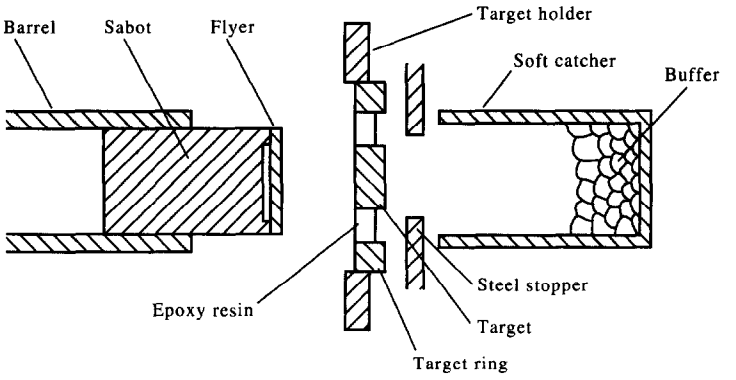

Fig. 2. Schematic of a light gas gun.

to the fracture of particles. The profiles of fractured particles are mostly perpendicular to the direction of propagation of stress waves. Figure 5 shows that the fracture develops from the fringe of particles into their interior. Figure 6 demonstrates the measured normalized number density distributions ρ of both fractured particles and all particles, defined as $\rho(c) = n(c)/\int_0^\infty n(c)\mathrm{d}c$, where c is the equivalent diameter of fractured particles or all particles. $n\mathrm{d}c$ is the number density of particles, whose equivalent diameters are between $c - c + \mathrm{d}c$. Two distributions are qualitatively similar to each other. In addition, the locations of their peaks in the two curves are in the same range, i.e. 2–5 μm. The positions of fractured particles in impacted specimens were examined with a Neophot 21 microscope and number of fractured particles on grain boundaries and inside grains were counted carefully. The area of observed fields was 0.7296 mm^2. Three groups of experiments give out nearly the same results. The average measured number density of fractured particles on grain boundaries was 135 per mm^2 and that inside grains was 64 per mm^2, the relative deviations are less than $\pm 5\%$. Therefore, the ratios of fractured particles on grain boundaries and inside grains were 13 and 2.5% respectively. The results indicated that the more probable positions of microcracks nucleation are junctions between grain boundaries and particles. This situation is typically presented in Fig. 7.

From the observed results, two questions should be answered. The first is why nucleation of microcracks is due to fracture of particles? The second is why normalized number density distribution of microcracks is qualitatively similar to that of particles?

For the purpose of comparison, the *in situ* uniaxial tensile were conducted with a Hitachi S-570 scanning electron microscope equipped with a tensile stage. The tensile specimen comes from the same aluminium alloy and dimensions of specimens are shown in Fig. 8. Figure 9 shows that nucleation of microcracks appeared in different ways, such as fracture of particles, debonding of phase boundaries between the matrix and particles and fracture of aluminium matrix by slip of grain boundaries, etc. Obviously the static case is very different from the concerned dynamic case.

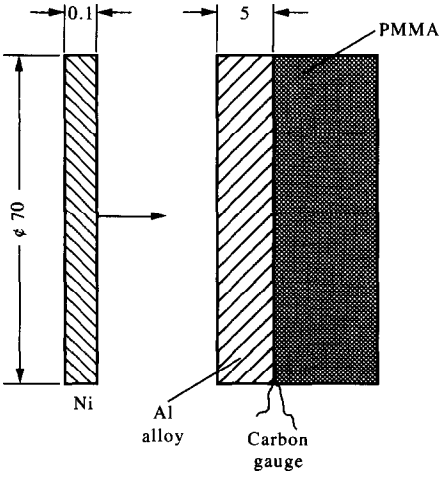

Fig. 3. The arrangement of carbon gauge.

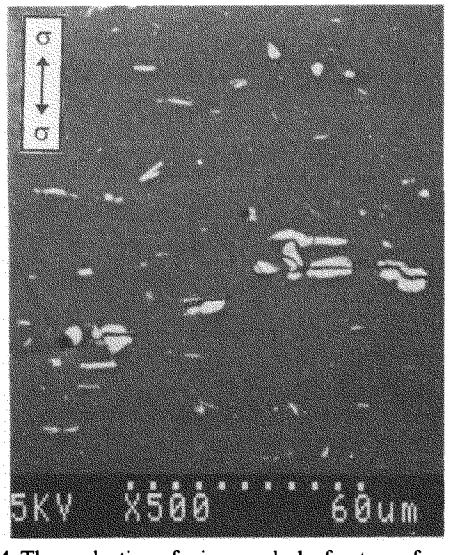

Fig. 4. The nucleation of microcracks by fracture of particles (σ = 7470 MPa, ΔT = 112 ns).

Fig. 5. The nucleation develops from the fringe of the particles into their interior ($\sigma = 7470$ MPa, $\Delta T = 112$ ns).

3. EMBRYO-DAMAGE INDUCED NUCLEATION

There is now some knowledge that nucleation of microdamage generally occurs at heterogeneities of materials, such as grain boundaries, phase boundaries or junctions of grain boundaries and phase boundaries. For one-dimensional strain state in planar impact tests, in addition to its high strain rate, the triaxial stress is much higher than shear stress. So that the mechanism of nucleation of microdamage might be the vacancy clustering. In this respect, the critical size for initial damage growing rather than vanishing was suggested by Raj and Ashby [1]

$$r_c = \frac{2\gamma}{\sigma_n} \tag{1}$$

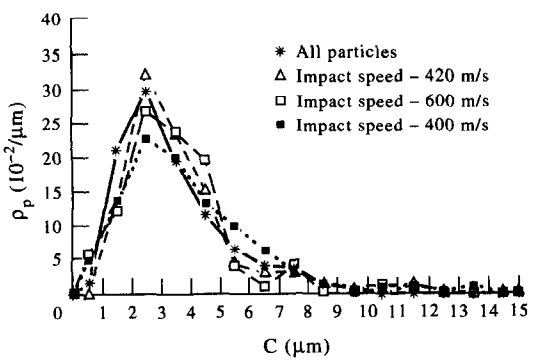

Fig. 6. The measured normalized number density distribution of both microcracks and particles.

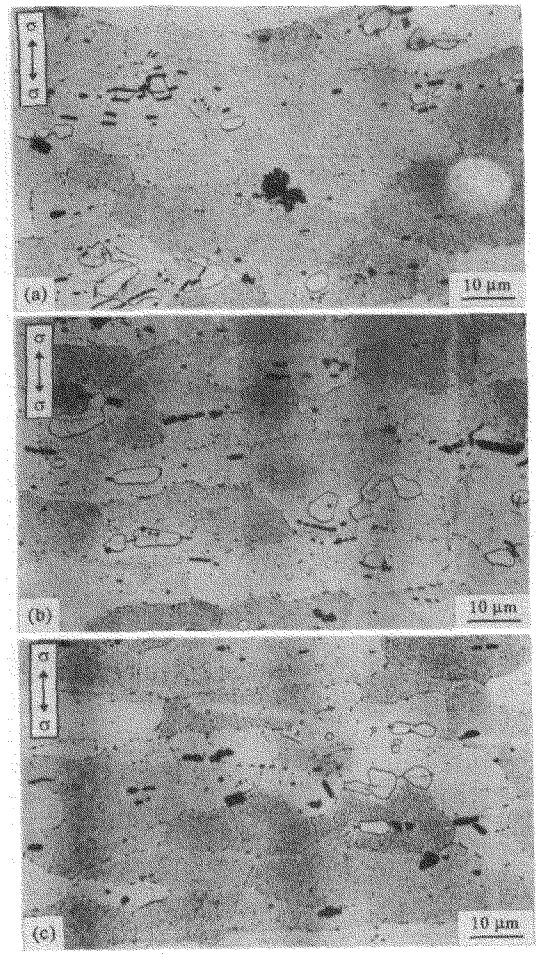

Fig. 7. The nucleation positions in dynamic case [(a) $\sigma = 7470$ MPa, $\Delta T = 112$ ns; (b) $\sigma = 5112$ MPa, $\Delta T = 115$ ns; (c) $\sigma = 4870$ MPa, $\Delta T = 142$ ns].

where r_c is critical size of stable cavities, γ is surface energy, σ_n is tensile stress. The surface energy can be estimated by Gilman's formula

$$\gamma \cong \frac{Ey}{\pi^2} \cong \alpha E \tag{2}$$

where E is Young's modulus, y is atomic spacing, $y \sim 10^{-10}$ m. So $\alpha \sim 10^{-11}$ m.

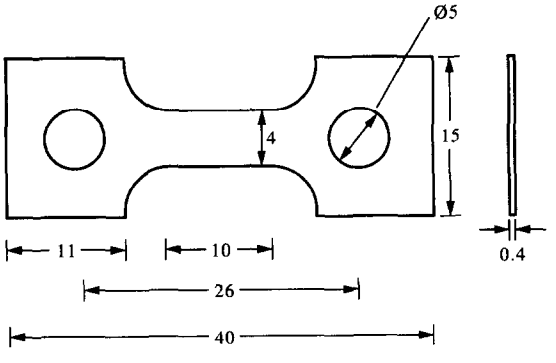

Dimensions of specimen (mm)

Fig. 8. Dimensions of specimen (mm).

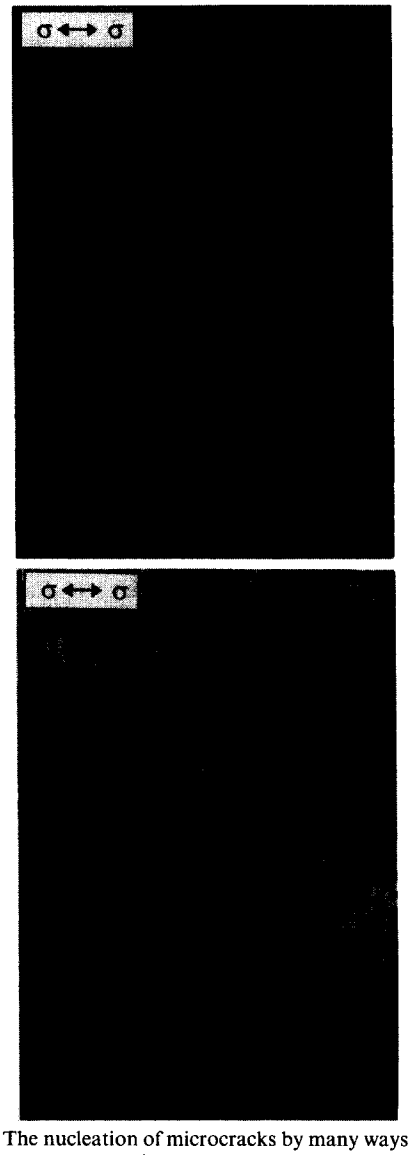

Fig. 9. The nucleation of microcracks by many ways in static tension ($\sigma = 420$ MPa).

Since there is no exact method to determine the mechanical properties of microscopic structures of materials, we have to appeal to some alternative approximation. Gilman's experimental results have shown that the ratio of the Young's modulus of different microstructures is approximately equal to the ratio of their micro-hardnesses [5]. So, the Young's modulus of a microstructure could be derived. For aluminium matrix, the Young's modulus $E_M \simeq 70$ GPa, hence for particles, the Young's modulus $E_I \simeq 2.11 E_M \simeq 148$ GPa. Therefore, the surface energy of matrix and particles can be estimated as

$$\gamma_I \cong \alpha E_I \simeq 1.48(\mathrm{J/m^2}) \tag{3}$$

$$\gamma_M \cong \alpha E_M \simeq 0.7(\mathrm{J/m^2}). \tag{4}$$

The energy consumed to debond particles from the matrix is

$$\gamma_D = \gamma_I + \gamma_M - \gamma_{I-M} \simeq 1.40\ (\mathrm{J/m^2}) \tag{5}$$

where $\gamma_{I-M} = |\gamma_I - \gamma_M| \simeq 0.77(\mathrm{J/m^2})$ is due to Antonov's law.

The critical size of cavities can be calculated by equation (1) with the experimental data of γ_M, γ_I and σ_n (4.87–7.47 GPa).

$$r_{Mc} = \frac{2\gamma_M}{\sigma_n} \simeq 0.3\text{–}0.2\ \mathrm{nm}$$

$$r_{Ic} = \frac{2\gamma_I}{\sigma_n} \simeq 0.6\text{–}0.4\ \mathrm{nm}. \tag{6}$$

It should be noted that these critical sizes of initial microdamages are too small to form any observed nucleated microcracks in micrometres in the tests. So, we defined these initial microdamage as "embryo-damage". It should also be noted that this embryo-damage controlled by diffusion must have enough incubation time to form. Now let us examine the timing of the small embryo-damage inside grains and particles, on grain boundaries and phase boundaries or at the junctions of grain boundaries and particles. Raj and Ashby [1] have indicated that the incubation time to the embryo-damage on boundaries is much shorter than any other cases. Therefore, the initial nucleation should occur on boundaries. They have given an approximate formula of the incubation time as follows

$$t_i \cong \frac{r_c^3 F_v}{4\sigma D_B} \tag{7}$$

where F_v is a geometrical parameter. For boundaries $F_v^a = 10^{-1} \sim 10^{-2}$, and for junctions of grain boundaries and particles, $F_v^b = 10^{-4} \sim 10^{-5}$. δD_B is the product of the diffusion parameter and the thickness of grain boundaries, and is approximately equal to $9.4 \times 10^{-15} \exp(-31.843)$ $(\mathrm{m^3\,s^{-1}})$ for aluminium alloy at room temperature [6]. So, the incubation time for the embryo-damage on boundaries is

$$t_i \cong \frac{r_{Mc}^3 F_v^a}{4\delta D_B} \sim 10^2\ \mu\mathrm{s} \tag{8}$$

whereas the incubation time for embryo-damage at the junctions of grain boundaries and particles is

$$t_i \cong \frac{r_{Mc}^3 F_v^b}{4\delta D_B} \sim 10^{-1}\ \mu\mathrm{s}. \tag{9}$$

As mentioned before, the durations of the impact tests are of 10^{-1} μs. By comparing the two incubation times of cavities on boundaries and at junctions of grain boundary and particles, one should conclude that the probability of forming the embryo-damage at junctions of grain boundaries and particles would be higher than that on boundaries under submicrosecond stress pulses. The other corroborative evidence is that in static tension all the incubation times to nucleate cavities on grain boundaries and phase

boundaries are short enough in comparison with the loading times. In fact, as mentioned in Section 2, various nucleations do occur in the static test. This situation was clearly shown in Fig. 9.

Since the size of embryo-damage is just several atomic spacings, they can not affect macroscopic properties of the material apparently. Hence, we should find out whether this embryo-damage at junctions of grain boundaries and particles can grow up in a fast way, and if it can, which growing path should be the most favorable one.

Of course, energy consumed to debond particles γ_D is close to γ_I, and less than γ_M. But one has to consider that the additional plastic energy consumed in the ductile aluminium matrix should be much greater than the surface energy, during the debonding and the fracture of the matrix. So, the fast brittle fracture of particles should be the less energy-consuming mechanism of microdamage nucleation.

As is well known, the cavities would cause stress concentration of about twice (45/22 see [7]) as great as the tensile stress around themselves, i.e. $\simeq 2 \cdot \sigma_n \sim 10^1$ GPa $\sim E_I/10$, namely, the stress around a cavity is the same order of magnitude of theoretical ultimate stress for brittle particles. So that this stress concentration might be the reason for the fracturing of particles. Figure 5 shows some evidence of this case. But, we should examine the condition to complete fracture of particles. This can estimated by comparing the energies before and after the fracture of particles.

$$U_0 = 0, \text{ initial}$$

$$U_t = \frac{-8(1-\nu^2)\sigma_n^2 a^3}{3E_I} + 2\pi a^2 \gamma_I \text{ fractured}$$

where ν is Poisson ratio and a is the radius of particle. $\nu \cong 0.31$ for the aluminium alloy.

Suppose that a brittle particle can be completely fractured only when

$$U_t \leqslant U_0$$

then, the size of brittle particles to fracture should be satisfy

$$d = 2a \geqslant \frac{4\pi\gamma_I \cdot 3E_I}{8(1-\nu^2)\sigma_n^2} \simeq 0.02 - 0.05\ \mu\text{m}.$$

The expression illustrates that the size of completely fractured particles should be larger than 0.02–0.05μm. In our experiments, the fractured particle observed with a microscope was in the range of 0.22–24.50 μm, this may be one reason of why there was not an obvious threshold of cracking size observed with the microscope.

So, the mechanism of the fracture of brittle particles on grain boundaries by small cavities was termed as the embryo-damage induced nucleation.

In the light of the equal opportunity for particles on grain boundaries to fracture, the phenomenon of equal probability of all observed particles to fracture, i.e. the same normalized number density distributions of fractured particles and all particles, is understandable.

4. CONCLUSION

The nucleation mechanism of microdamage of an aluminium alloy under impact loading was explored by the experimental observation, metallographic measurements and theoretical analysis. Some essential facts and ideas could be derived as follows:

1. The most probable nucleation of microdamage in the aluminium alloy under impact loading is fracture of brittle particles on grain boundaries.
2. The concept of embryo-damage induced nucleation can explain the observed facts properly, including the position and timing of nucleation as well as the fact that the normalized density distribution of fractured particles is coincided with that of all particles.

Acknowledgements—This work was supported by the National Science Foundation of China and the Chinese Academy of Sciences under special grant KM 85-33. The authors are indebted to Professor L. T. Shen for his valuable help and suggestions in accomplishing this work.

REFERENCES

1. R. Raj and M. F. Ashby, *Acta metall.* **23,** 653 (1975).
2. R. G. Fleck, D. M. R. Taplin and C. J. Beevers, *Acta metall.* **23,** 415 (1975).
3. D. R. Curran, L. Seaman and D. A. Shockey, *Phys. Repts* **147,** 977 (1987).
4. J. Gurland, in *Quantitative Microscopy* (edited by R. T. Dehoff and F. N. Rhines), p. 278. McGraw-Hill, New York (1968).
5. J. J. Gliman, in *The Science of Hardness Testing and Its Research Applications* (edited by J. H. Westbrook and H. Conrad), p. 35. ASM (1973).
6. A. M. Brown and M. F. Ashby, *Acta metall.* **28,** 1085 (1980).
7. S. P. Timoshenko and J. N Goodier, *Theory of Elasticity (Third edition)*, p. 398. McGraw-Hill, New York (1970).